LJMU Research Online

Sabino, CP, Wainwright, M, Dos Anjos, C, Sellera, FP, Baptista, MS, Lincopan, N and Ribeiro, MS

 Inactivation Kinetics and Lethal Dose Analysis of Antimicrobial Blue Light and Photodynamic Therapy.

http://researchonline.ljmu.ac.uk/id/eprint/11269/

Article

For more information please contact researchonline@ljmu.ac.uk

Inactivation Kinetics and Lethal Dose Analysis of Antimicrobial Blue Light and Photodynamic Therapy

Caetano P. Sabino[1,2], Mark Wainwright,[3] Carolina dos Anjos[4], Fabio P. Sellera[4], Maurício S. Baptista[5], Nilton Lincopan[2,6], and Martha S. Ribeiro[7]

[1]*BioLambda, Scientific and Commercial LTD, São Paulo, SP, Brazil*

[2]*Department of Clinical Analysis, School of Pharmaceutical Sciences, University of São Paulo, São Paulo, SP, Brazil*

[3]*School of Pharmacy & Biomolecular Sciences, Liverpool John Moores University, Liverpool, UK*

[4]*Department of Internal Medicine, School of Veterinary Medicine and Animal Science, University of São Paulo, São Paulo, SP, Brazil*

[5]*Department of Biochemistry, Institute of Chemistry, University of São Paulo, São Paulo, SP, Brazil*

[6]*Department of Microbiology, Institute for Biomedical Sciences, University of São Paulo, São Paulo, SP, Brazil*

[7]*Center for Lasers and Applications, Nuclear and Energy Research Institute, National Commission for Nuclear Energy, São Paulo, SP, Brazil*

21 **ABSTRACT**

22 **Background:** Photodynamic therapy (PDT) has been long used to treat localized

23 tumors and infections. Currently, microbial inactivation data is reported presenting

24 survival fraction averages and standard errors as discrete points instead of a

25 continuous curve of inactivation kinetics. Standardization of this approach would

26 allow clinical protocols to be introduced globally, instead of the piecemeal situation

27 which currently applies.

28 **Methods:** To this end, we used a power-law function to fit inactivation kinetics and

29 directly report values of lethal doses (LD) and a tolerance factor (T) that informs if

30 inactivation rate varies along the irradiation procedure. A deduced formula was also

31 tested to predict LD for any given survival fraction value. We analyzed the

32 photoantimicrobial effect caused by red light activation of methylene blue (MB-

33 APDT) and by blue light (BL) activation of endogenous microbial pigments against 5

34 clinically relevant pathogens.

35 **Results:** Following MB- APDT, *E. coli* and *S. aureus* cells become increasingly

36 more tolerant to inactivation along the irradiation process (T<1). *K. pneumoniae*

37 presents opposite behavior, *i.e.*, more inactivation is observed towards the end of the

38 process (T>1). *P. aeruginosa* and *C. albicans* present constant inactivation rate

39 (T~1). In contrast, all bacterial species presented similar behavior during inactivation

40 caused by BL, *i.e.*, continuously becoming more sensitive to blue light exposure

41 (T>1).

42 **Conclusion:** The power-law function successfully fit all experimental data. The

43 analytical model precisely predicted LD and T values. We expect that these

44 analytical models may contribute to more standardized methods for comparisons of

45 photodynamic inactivation efficiencies.

46

47 ***Keywords:*** bacteria; fungi; mathematical analysis; microbial control;

48 photoantimicrobial; photoinactivation; photodynamic antimicrobial chemotherapy.

49

Introduction

Photodynamic therapy (PDT) has been long studied and used to treat localized tumors and infections [1, 2]. This light-based technology platform produces cytotoxic molecular species in a space-time controlled manner, *i.e.,* in the absence of light, photosensitizer (PS) or oxygen, photodynamic reactions do not occur. The light-excited PS interacts with molecular oxygen, either by charge (type I reaction) or energy donation (type II reaction), forming a variety of reactive oxygen species (ROS) that can destroy bacteria, parasites, fungi, algae and viral particles [2-7].

The use of PSs thus offers an effective local – not just topical – approach to infection control, often termed antimicrobial photodynamic therapy (APDT). Importantly, the agency of ROS here means that the conventional resistance status of the microbial target is unimportant. However, in order to provide photosensitization that is fit for purpose, the killing effects of PSs require proper quantification and benchmarking, *e.g.,* the PS concentration and light dose required to destroy a given microbial burden at a certain rate. Standardization of this approach would allow clinical protocols to be introduced globally, instead of the piecemeal situation which currently applies.

According to the Second Law of Photochemistry, for each photon absorbed by a chemical system, only one molecule can be excited and subsequently undergo a photochemical reaction. Based on this principle, current literature supports photodynamic dosimetry in respect of the number of absorbed photons (*Absorbed Photons*/cm^3 instead of J/cm^2) to provide a rather interpretable comparison of PS efficiency [8, 9]. It has been proposed that using this method, problematic dosimetry due to variable PS concentration, optical path and excitation wavelength band can be minimized. However, some other problematic situations can be addressed by this method as well. If a filter effect is caused either by high cellular and/or PS concentrations, absorbed photon results may lead to divergent interpretations. Also, Prates *et al.* [10] have demonstrated that if the number of absorbed photons is kept constant but irradiance varies, the level of microbial inactivation also diverges [10]. These situations suggest the need for a more robust standard method, even though the number of absorbed photons per unit volume can be considered to represent an improvement on merely reporting inactivation as a function of radiant exposure.

83   Currently, the most accepted form of reporting microbial inactivation data in
84   scientific articles is presenting survival fraction averages and standard errors as
85   discrete points instead of a continuous curve of inactivation kinetics [9, 10]. However,
86   analysis of variance over individual points only allows the interpretation of whether
87   those points present statistically significant differences among themselves.
88   Therefore, if one intends to compare the potency of a set of variable antimicrobial
89   photodynamic systems (*i.e.,* different PSs, microbial species, light sources, etc.) this
90   analysis may be misguided by local observation of a single point instead of the
91   interpretation of a global kinetics rate. Therefore, this analytical method may lead to
92   false-positive or -negative interpretations in respect to the overall phenomena of
93   microbial inactivation kinetics.

94   To this end, we report a simple mathematical analysis of continuous bacterial
95   inactivation kinetics curves. We analyzed the photodynamic killing effect caused by
96   red light activation of methylene blue (MB) and by blue light activation of
97   endogenous microbial photosensitive pigments. We expect that this method may
98   assist in developing standardized and more insightful analysis of photoantimicrobial
99   systems.

100

101   **Material and Methods**

102

103   ***APDT experiments***

104   In the present study we used the following strains from the American Type
105   Culture Collection (ATCC): *Escherichia coli* (ATCC 25922), *Staphylococcus aureus*
106   (ATCC 25923), *Klebsiella pneumoniae* (ATCC 700603), *Pseudomonas aeruginosa*
107   (ATCC 27853) and *Candida albicans* (ATCC 90028).

108   Standard APDT susceptibility testing was carried out based on Prates *et al.*
109   [10]. Inocula were prepared from log-phase overnight cultures. The turbidity of cell
110   suspensions was measured in a spectrophotometer to obtain inocula at McFarland
111   scale 0.5. The scale was calibrated to obtain an optical density of 0.09 at 540 nm and
112   625 nm resulting in 1-2 x 10^6 CFU/mL of fungi cells, and 1-2 x 10^8 CFU/mL of
113   bacterial cells, respectively. Inocula were diluted to a working concentration of 1-2 x
114   10^5 CFU/mL of fungi or 1-2 x 10^7 CFU/mL of bacteria.

115   MB hydrate (purity > 95%, Sigma-Aldrich, USA) was employed as the
116   exogenous PS for this study. Before irradiation, cells were incubated with 100 µM of

117   MB in phosphate-buffered saline (PBS) for 10 min at room temperature and in the

118   dark, to allow initial uptake. One-mL aliquots were individually placed in clean wells

119   of a 12-well microplate. To avoid cross light exposure, each sample was kept in

120   individual microtubes in the dark during pre-irradiation time and placed in the 12-

121   wells plate only for irradiation.

122   A red LED probe (660 ± 10 nm, Prototype 1, BioLambda, Brazil) was

123   positioned perpendicularly above each sample, keeping the beam diameter at the

124   bottom of the well at 25 mm (which coincides to a single well diameter from the 12-

125   wells plate). Red light irradiance was kept constant at 100 mW/cm^2 and radiant

126   exposure levels varied according to each microbial species sensitivity to MB-APDT

127   as previously determined in pilot experiments.

128   A blue LED irradiator (415 ± 12 nm, LEDbox, BioLambda, Brazil) was placed

129   below 12-well plates containing 1 mL of each microbial sample. In this case, no

130   exogenous PS was added to the systems. Blue light irradiance was kept constant at

131   38.2 mW/cm^2. Radiant exposure levels varied according to each microbial species

132   sensitivity to blue light inactivation as previously determined in pilot experiments.

133   Immediately after each irradiation process, bacterial suspensions were serially

134   diluted in PBS to give dilutions from 10^{-1} to 10^{-6} times the original concentration. Ten-

135   µL aliquots of each dilution were streaked onto Mueller-Hinton agar plates, in

136   triplicate, and incubated at 37° C overnight. A similar procedure was performed for

137   fungi. However, in this case dilutions were between 10^{-1} - 10^{-4}-fold and streaked onto

138   Sabouraud dextrose agar. The colonies were counted and converted into CFU/mL

139   for survival fraction analysis.

140

141   ***Data analysis***

142   We adapted a power law function to fit inactivation kinetics data in respect to

143   variable radiant exposure levels (**equation 1**). Theoretical lethal dose (LD) for any

144   given inactivation rate (*i.e.,* % of bacterial survival fraction) was calculated according

145   to **equation 2**. Fitting, residuals and derivatives were calculated using the Prism 7.0

146   (GraphPad, USA) interface.

$$log_{10}\left(\frac{N_0}{N}\right) = \left(\frac{Dose}{LD_{90}}\right)^{T}$$

Equation 1

$$LD_i = LD_{90} \left(-log_{10} \left(1 - \frac{i}{100} \right) \right)^{1/T} \qquad \textbf{Equation 2}$$

147   where:

148   N_0= initial microbial burden; N= final microbial burden; *Dose*= light exposure (*e.g.* J,

149   J/cm^2, time units, *Absorbed Photons*/cm^3, etc.); LD_{90}= lethal dose for 90% of

150   microbial burden (in light exposure units); T= tolerance factor; i= inactivation

151   percentage (%).

152

153   Unfortunately, data analysis softwares may not have **equations 1-2** as

154   standard models for fitting data. In Prism 7.0, we added **equation 1** as an explicit

155   equation for non-linear regression (curve fit) analysis in the following formula:

156   Y=(x/LD$_{90}$)^(T). Initial values for data fit of LD$_{90}$ and T were set as 1. LDs were

157   calculated by Microsoft Excel 2018 using LD$_{90}$ and T values obtained from equation

158   1. The LD$_{99.9}$ and LD$_{100}$ values were then calculated for each dataset using equation

159   2 in the following formula: =(LD$_{90}$)*(-LOG$_{10}$(1-(i/100)))^(1/T).

160   Experiments were performed at least in triplicates. Quantitative data are

161   presented as log$_{10}$ of normalized means and standard error of means calculated in

162   relation to the respective control groups. Survival fraction data were analyzed by

163   Shapiro-Wilk test to confirm normality. Fitted curves were analyzed using F-test to

164   check if any of the fitted curves are shared in between different species. Lethal-dose

165   and T value analysis were compared in between species using one-way analysis of

166   variance (ANOVA) with Bonferroni as post-hoc test for multiple comparisons. Results

167   were considered significant if $p < 0.05$.

168

169   **Results and Discussion**

170

171   The Weibull analysis is a well-known and accepted statistical method that

172   uses a power-law function to describe breakdown kinetics of various materials. This

173   analysis assumes that the survival curve is affected by cumulative distributions of

174   damages that leads to lethal effects. Here we assumed that it properly describes

175   effects such as the cumulative oxidative damage imposed by APDT over living cells

176   [11].

177 Historically, this statistical model has been mostly employed in industries,
178 such as aerospace and automotive, to estimate the reliability on lifespan of
179 mechanical parts [12]. This mathematical function has been used to describe bacterial
180 inactivation kinetics during thermal inactivation or gamma radiation, UV- and blue-
181 light irradiation, free of exogenous PSs [13-16]. However, it has not so far been
182 proposed as a method to standardize APDT sensitivity protocols.

183 Power-Law fit appears to represent a very good description for APDT
184 inactivation kinetics of our data. Adjusted R^2 values always fluctuated above 0.95
185 (**Table 1**). These values represent very good results in relation to general non-linear
186 curve fittings.

187

188 **Table 1.** Adjusted R^2 value of each non-linear curve fit

| Species	E. coli	S. aureus	P. aeruginosa	K. pneumoniae	C. albicans
MB-APDT	0.9745	0.9955	0.9939	0.9834	0.9793
Blue Light	0.9691	0.9518	0.9805	0.9526	0.9756

189

190 The F-test applied over non-linear regressions reported that each species
191 dataset presents a unique inactivation kinetics curve (**fig. 1a-b**). This means that
192 even though some inactivation data points may not present statistical differences in
193 between species, the entire inactivation kinetics are not the same.

194 The first derivative of inactivation curves (**fig. 1c-d**) further illustrates the
195 variation in inactivation rates. This analysis shows how fast the inactivation occurs
196 during the irradiation procedure. For MB-APDT, *E. coli* and *S. aureus* cells are
197 inactivated rapidly in the beginning of the procedure but slower towards the end of
198 the process. *K. pneumoniae* presents the exact opposite behavior. *P. aeruginosa*
199 and *C. albicans*, however, present almost a constant inactivation rate. On the other
200 hand, all bacterial species presented similar behavior during inactivation caused by
201 blue light alone, i.e., slow initial inactivation but becoming continuously more
202 sensitive to blue light exposure. Conversely, *C. albicans* presented again almost a
203 constant inactivation rate.

204
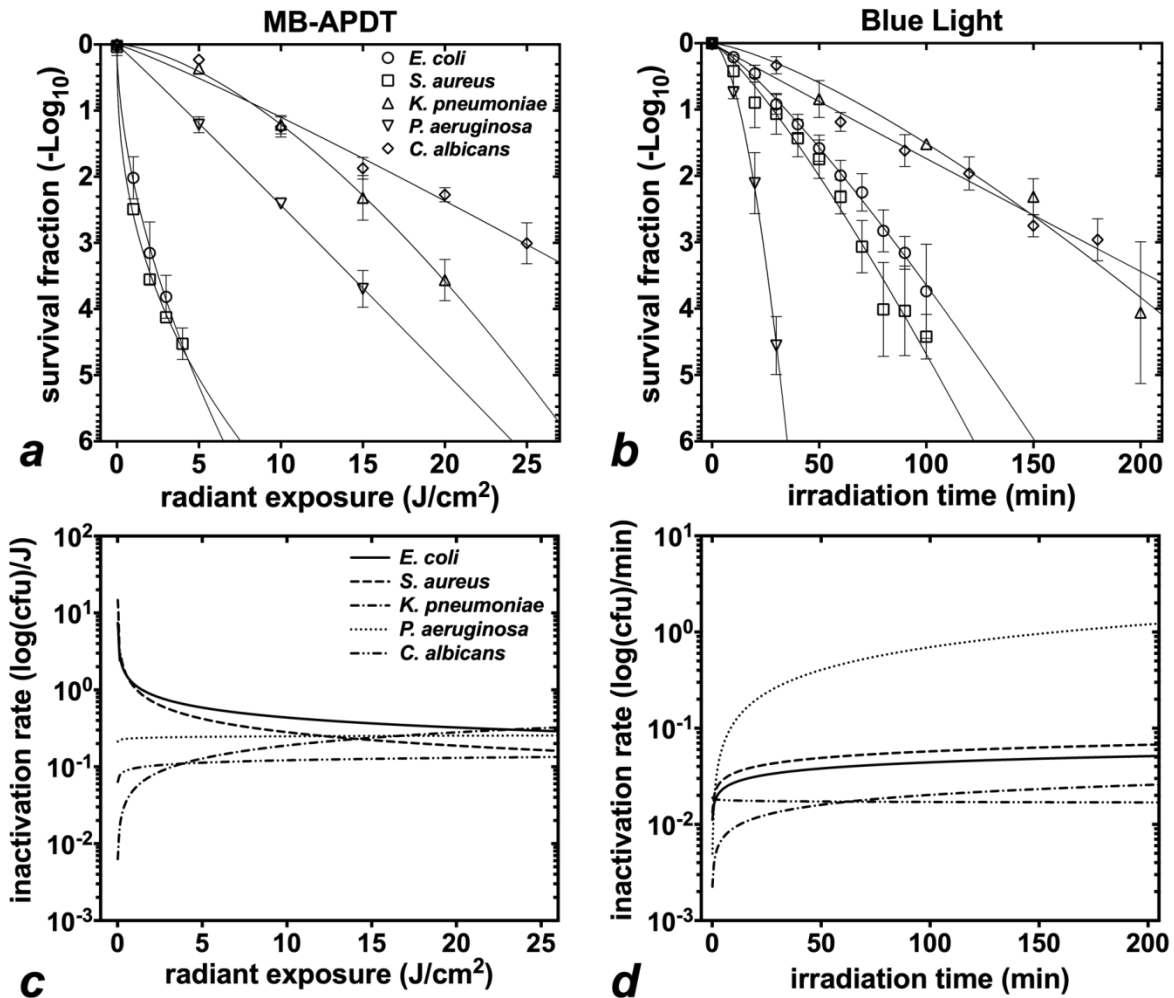
Figure 1. Inactivation kinetics plots. On the top, survival fraction values are presented for (*a*) MB-APDT and (*b*) blue light photoinactivation. Below are the first derivatives (i.e., microbial inactivation rate) of each non-linear regression curves fitted for (*c*) MB-APDT and (*d*) blue light photoinactivation. The experimental data from *a* and *b* are the log reduction of normalized survival fraction and standard errors.

We also submitted inactivation data to double-log transformations in order to confirm data linearization. This is a standard empirical method used to confirm the feasibility of a power-law fit in experimental datasets. As a matter of fact, successful linearization (**fig. 2a-b**) further proves the ability to describe photoinactivation kinetics assuming a Power-Law behavior, yet all residual dispersions presented random distributions (**fig. 2c-d**).
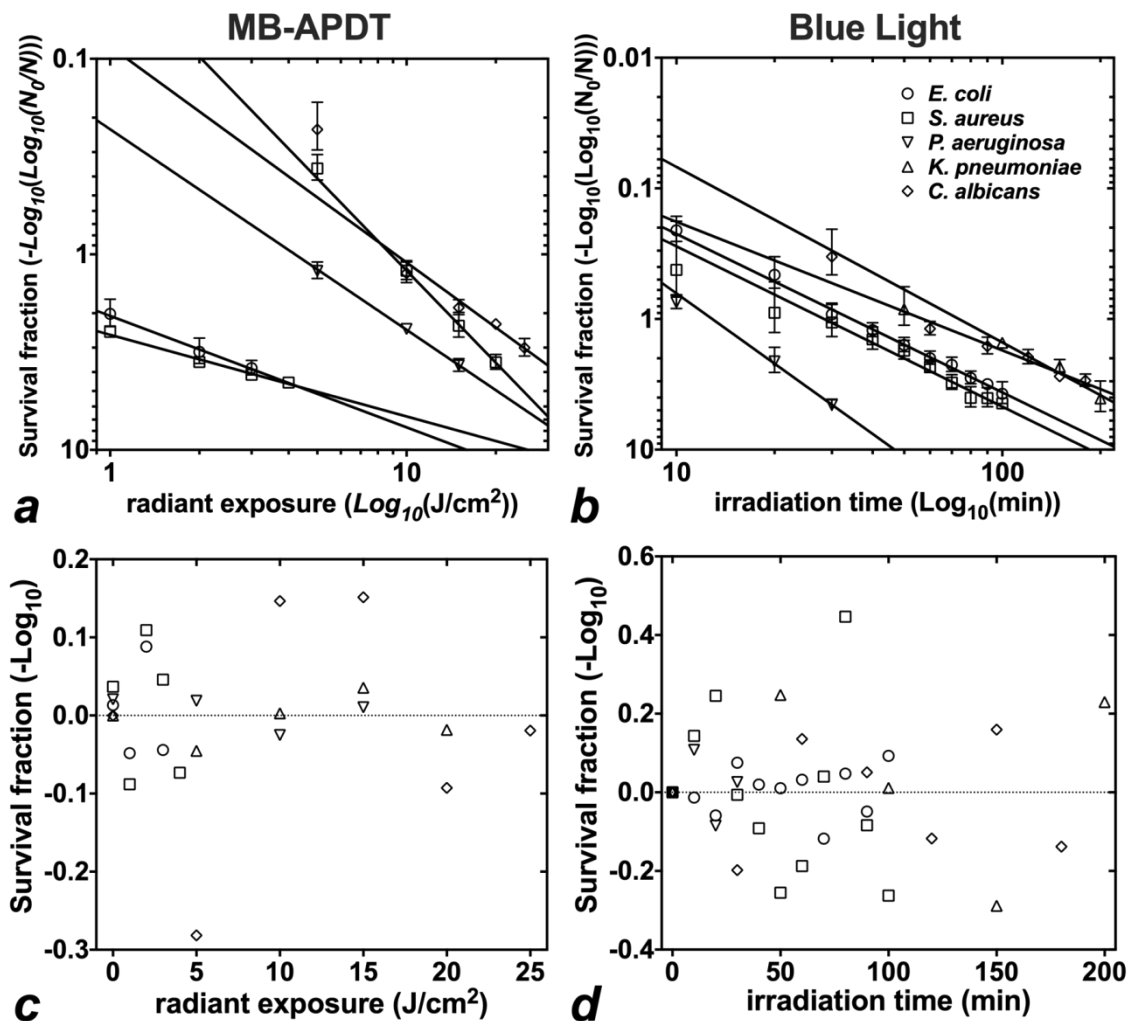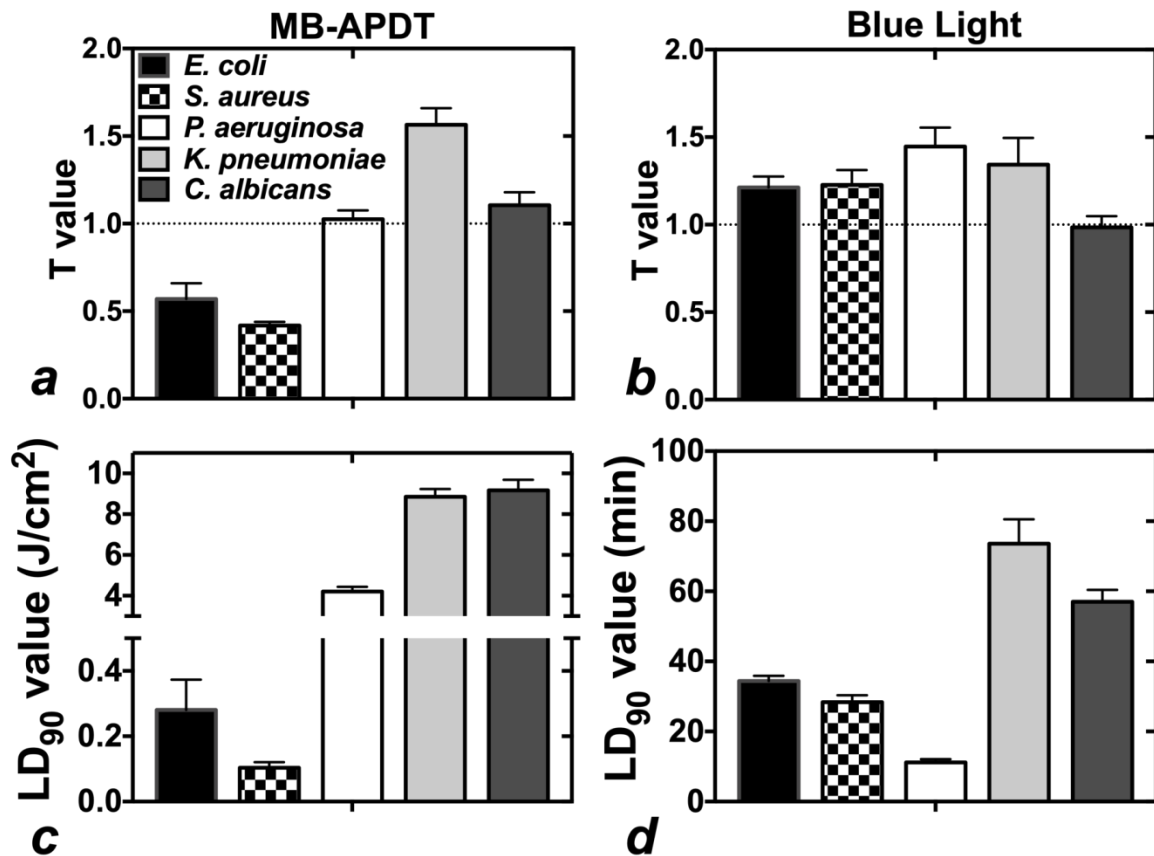
Figure 2. Linearization of inactivation kinetics data by double-log transformations in *a* and *b* confirms the hypothesis of power law function fitting. Residuals of fitted data in *c* and *d* presented random distributions around the average, confirming data homogeneity and normality.

Non-linear regression results are presented in **figure 3** as values of the tolerance factor T and lethal doses for 90 percent ($1log_{10}$) of inactivation. The tolerance factor T informs the concavity of the inactivation curves; if T>1, cells are initially tolerant to APDT but become increasingly sensitive; if T<1, cells are initially very sensitive, but some persistent cells remain more tolerant to inactivation. Hence, the behavior observed at the inactivation rate curves (**fig. 1c-d**) can be indicated by the T values (**fig. 3a-b**).

For MB-APDT (**fig. 3a**), *S. aureus* and *E. coli* T<1 with no statistically significant difference among themselves; *P. aeruginosa* and *C. albicans* presented T

values close to 1, with no statistical difference among themselves; *K. pneumoniae* presented a T value close to 1.5 and was statistically different from all other species treated by MB-APDT. For blue light inactivation, all species presented T values above 1, without any statistically significant differences in between them. These statistical analysis results are presented in **tables 2-3** in supplementary material.


Figure 3. Non-linear regression parameters of inactivation kinetics obtained for each tested species. On the top, T values are presented for (***a***) MB-APDT and (***b***) blue light photoinactivation. Below are the LD90 values calculated for (***c***) MB-APDT and (***d***) blue light photoinactivation. The presented values are means of constants and standard errors directly obtained by power law non-linear regressions.

Lethal doses for 90% (*i.e.*, 1 $\log_{10}$) inactivation with MB-APDT (**fig. 3c**) show that *E. coli* and *S. aureus* are the most sensitive and present statistically significant differences to all other species but not among themselves. *P. aeruginosa* presented an intermediate sensitivity to MB-APDT that was significantly different from all other species. *K. pneumoniae* and *C. albicans* are significantly more tolerant to MB-APDT

than all other species but not amongst themselves. Even though no statistical differences were observed for T values of blue light inactivation (**fig. 3d**), several particularities were reported for lethal dose values. *E. coli* and *S. aureus* are quite sensitive to blue light and present statistically similar behavior. However, *P. aeruginosa* seems to be the most sensitive species tested to blue light, although it did not show statistically significant differences relative to *S. aureus*. Such high sensitivity of *P. aeruginosa* to blue light may be linked to high yield production of pyoverdine, a naturally occurring fluorescent pigment that strongly absorbs 415 nm light and may undergo photodynamic reactions [17, 18]. *K. pneumoniae* and *C. albicans* are significantly the most tolerant species to blue light and do not present statistical differences between themselves. These statistical results can be seen in **tables 4-5** from supplementary material.

The concept of inactivation rate illustrated by the first derivative of inactivation curves can be specifically quantified by the tolerance factor, presented as T values (**fig. 3a**). This is a dimensionless value that indicates the overall inactivation rate behavior. It describes whether cells are more tolerant to inactivation at the beginning of the irradiation process or at the end. Therefore, we can indicate the existence of microbial species with a constitutive tolerance (T>1) that is soon depleted making cells become increasingly sensitive (*e.g.,* MB-APDT for *E. coli* and *S. aureus*); or the presence of adapting or more persistent cells (T<1) that remain harder to kill after a period of irradiation (*e.g.,* blue light for bacteria). Microbial species with T values close to unity may represent an intermediate situation (*e.g.,* *C. albicans* in both situations). The exact tolerance mechanisms responsible for these inactivation kinetics variations may have a multifactorial basis that leads to a constant inactivation rate.
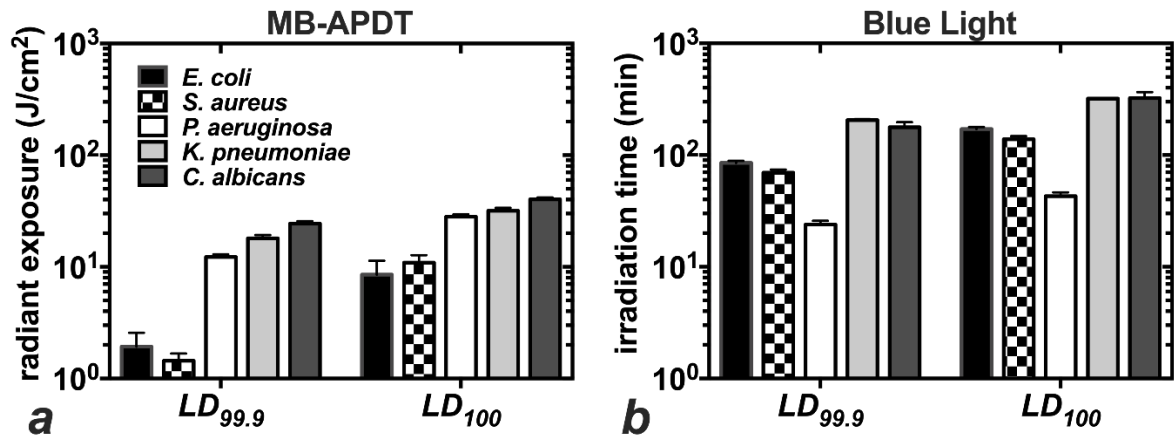
Figure 4. Lethal dose values calculated for 99.9% ($3\log_{10}$) and 100% ($7\log_{10}$ for bacteria and $5\log_{10}$ for yeast). On the left (**a**), calculated lethal doses are presented for MB-APDT groups and on the right (**b**) they are presented for blue light inactivation. The presented values are means and standard errors obtained from data of at least three independent experiments.

A very useful aspect of using our proposed model is the ability to calculate lethal doses for any given level of survival fraction. Such information allows precise and direct comparisons in between experimental groups and also provides basis for future experimental planning. For example, if one is interested to analyze perspectives of microbial inactivation by APDT or blue light of different experimental groups at the same survival fraction level, this analysis can be used to establish the required light doses. Alternatively, this analysis can also calculate the dose required to achieve complete microbial inactivation (*i.e.,* LD_{100}), which is experimentally inviable to measure. In **figure 4**, we used data obtained from **equation 1** (*e.g.,* LD_{90} and T values) to calculate $LD_{99.9}$ and LD_{100} through **equation 2**. As expected, experimental groups with $T < 1$ presented much greater variations in between $LD_{99.9}$ and LD_{100} than groups with $T > 1$. The statistical results respective to data from **figure 3** are presented in **tables 6-7** from supplementary material.

For experimental verification of our proposed model, we compared photodynamic inactivation kinetics of MB-APDT and blue light using diverse species of clinically relevant pathogens. MB currently is the most broadly PS used in APDT studies while blue light inactivation is a promising antimicrobial platform using novel high-powered blue LEDs. These surrogates represent very different approaches to light-mediated microbial control and, yet, equation 1 successfully fit all tested data.

We also showed that doses can be reported in time or energy units with no detriment of the analysis output. Thus, we expect that other PS classes should also be suitable for such analysis, and that this approach will allow the development of standardized protocols for photodynamic antimicrobial therapies. This way, future studies that choose to use our model could report quantitative data regarding LD_{90} and T values in order to allow comparative analysis in between different photoinactivation systems (*i.e.*, different PS, light sources, irradiances, etc.).

Conclusion

We reported a mathematical model to fit and describe photoinactivation kinetics in interpretative and quantitative terms. A power-law function successfully fit all data from experiments performed with MB-APDT and blue light alone. A deduced formula could also be used to precisely predict lethal doses for any given survival fraction value. We truly expect that these analytical methods may contribute to a more standardized protocol for comparisons of photodynamic inactivation efficiency.

Conflict of interest

C. P. Sabino is an associate at BioLambda but declares to only have scientific interest on this study. There are no further conflicts of interest to be declared.

References

1.   Agostinis P, Berg K, Cengel KA, Foster TH, Girotti AW, Gollnick SO, et al. Photodynamic therapy of cancer: an update. CA: A Cancer Journal for Clinicians 2011;61(4):250-81.

2.   Wainwright M. Photodynamic antimicrobial chemotherapy (PACT). The Journal of Antimicrobial Chemotherapy. 1998;42(1):13-28.

338   3.   Maisch T, Hackbarth S, Regensburger J, Felgentrager A, Baumler W,
339   Landthaler M, et al. Photodynamic inactivation of multi-resistant bacteria (PIB) - a
340   new approach to treat superficial infections in the 21st century. Journal der
341   Deutschen Dermatologischen Gesellschaft = Journal of the German Society of
342   Dermatology : JDDG. 2011;9(5):360-6.

344   4.   Dai T, Huang YY, Hamblin MR. Photodynamic therapy for localized infections-
345   -state of the art. Photodiagnosis and photodynamic therapy. 2009;6(3-4):170-88.

347   5.   Lyon JP, Moreira LM, de Moraes PC, dos Santos FV, de Resende MA.
348   Photodynamic therapy for pathogenic fungi. Mycoses. 2011;54(5):e265-71.

350   6.   Schmidt R. Photosensitized Generation of Singlet Oxygen. Photochemistry
351   and Photobiology. 2007;82(5):1161-77.

353   7.   Sellera FP, Sabino CP, Ribeiro MS, Gargano RG, Benites NR, Melville PA, et
354   al. *In vitro* photoinactivation of bovine mastitis related pathogens. Photodiagnosis
355   and Photodynamic Therapy. 2016;13:276-81.

357   8.   Wilson BC, Patterson MS, Lilge L. Implicit and explicit dosimetry in
358   photodynamic therapy: a New paradigm. Lasers in Medical Science. 1997;12(3):182-
359   99.

361   9.   Cieplik F, Pummer A, Regensburger J, Hiller KA, Spath A, Tabenski L, et al.
362   The impact of absorbed photons on antimicrobial photodynamic efficacy. Frontiers in
363   Microbiology. 2015;6:706.

365   10.   Prates RA, Silva EG, Yamada AM, Suzuki LC, Paula CR, Ribeiro MS. Light
366   parameters influence cell viability in antifungal photodynamic therapy in a fluence
367   and rate fluence-dependent manner. Laser Physics. 2009;19(5):1038-44.

369   11.   Weibull W. A Statistical Distribution Function of Wide Applicability. Journal of
370   Applied Mechanics-Transactions of The Asme. 1951;18(3):293-7.

372   12.   Weibull GW. Citation Classic - a Statistical Distribution Function of Wide
373   Applicability. Cc/Eng Tech Appl Sci. 1981(10):18-.

374

375   13.   Holcomb DL, Smith MA, Ware GO, Hung YC, Brackett RE, Doyle MP.
376   Comparison of six dose-response models for use with food-borne pathogens. Risk
377   Analysis 1999;19(6):1091-100.

378

379   14.   Hu X, Mallikarjunan P, Koo J, Andrews LS, Jahncke ML. Comparison of
380   kinetic models to describe high pressure and gamma irradiation used to inactivate
381   *Vibrio vulnificus* and *Vibrio parahaemolyticus* prepared in buffer solution and in
382   whole oysters. Journal of Food Protection. 2005;68(2):292-5.

383

384   15.   McKenzie K, Maclean M, Timoshkin IV, Endarko E, MacGregor SJ, Anderson
385   JG. Photoinactivation of bacteria attached to glass and acrylic surfaces by 405 nm
386   light: potential application for biofilm decontamination. Photochemistry and
387   Photobiology. 2013;89(4):927-35.

388

389   16.   Bozkurt H, D'Souza DH, Davidson PM. Determination of thermal inactivation
390   kinetics of hepatitis A virus in blue mussel (Mytilus edulis) homogenate. Applied and
391   Environmental Microbiology. 2014;80(10):3191-7.

392

393   17.   Elliott RP. Some properties of pyoverdine, the water-soluble fluorescent
394   pigment of the pseudomonads. Applied Microbiology. 1958;6(4):241-6.

395

396   18.   Propst C, Lubin L. Light-mediated changes in pigmentation of *Pseudomonas*
397   *aeruginosa* cultures. Journal of General Microbiology. 1979;113(2):261-6.

398

399

400   **Table 2.** One-way ANOVA results for comparisons of T values of MB-APDT

T value comparison	Significant?	Adjusted P Value
E. coli vs. *S. aureus*	No	>0,9999
E. coli vs. *P. aeruginosa*	Yes	0,0184
E. coli vs. *K. pneumoniae*	Yes	<0,0001
E. coli vs. *C. albicans*	Yes	0,0056

	Yes	0,0021
S. aureus vs. *P. aeruginosa*	Yes	0,0021
S. aureus vs. *K. pneumoniae*	Yes	<0,0001
S. aureus vs. *C. albicans*	Yes	0,0007
P. aeruginosa vs. *K. pneumoniae*	Yes	0,0031
P. aeruginosa vs. *C. albicans*	No	>0,9999
K. pneumoniae vs. *C. albicans*	Yes	0,0106

401

402

403 **Table 3.** One-way ANOVA results for comparisons of T values of blue light

T value comparison	Significant?	Adjusted P Value
E. coli vs. *S. aureus*	No	>0,9999
E. coli vs. *P. aeruginosa*	No	>0,9999
E. coli vs. *K. pneumoniae*	No	>0,9999
E. coli vs. *C. albicans*	No	>0,9999
S. aureus vs. *P. aeruginosa*	No	>0,9999
S. aureus vs. *K. pneumoniae*	No	>0,9999
S. aureus vs. *C. albicans*	No	>0,9999
P. aeruginosa vs. *K. pneumoniae*	No	>0,9999
P. aeruginosa vs. *C. albicans*	No	0,0831
K. pneumoniae vs. *C. albicans*	No	0,2932

404

405

406 **Table 4.** One-way ANOVA results for comparisons of LD_{90} values of MB-APDT

LD_{90} value comparison	Significant?	Adjusted P Value
E. coli vs. *S. aureus*	No	>0,9999
E. coli vs. *P. aeruginosa*	Yes	<0,0001
E. coli vs. *K. pneumoniae*	Yes	<0,0001
E. coli vs. *C. albicans*	Yes	<0,0001
S. aureus vs. *P. aeruginosa*	Yes	<0,0001
S. aureus vs. *K. pneumoniae*	Yes	<0,0001
S. aureus vs. *C. albicans*	Yes	<0,0001
P. aeruginosa vs. *K. pneumoniae*	Yes	<0,0001
P. aeruginosa vs. *C. albicans*	Yes	<0,0001
K. pneumoniae vs. *C. albicans*	No	>0,9999

407

408

409 **Table 5.** One-way ANOVA results for comparisons of LD_{90} values of blue light

LD value comparison	Significant?	Adjusted P Value
E. coli vs. *S. aureus*	No	>0,9999

E. coli vs. *P. aeruginosa*	Yes	0,0116
E. coli vs. *K. pneumoniae*	Yes	0,0002
E. coli vs. *C. albicans*	Yes	0,0141
S. aureus vs. *P. aeruginosa*	No	0,0771
S. aureus vs. *K. pneumoniae*	Yes	<0,0001
S. aureus vs. *C. albicans*	Yes	0,0025
P. aeruginosa vs. *K. pneumoniae*	Yes	<0,0001
P. aeruginosa vs. *C. albicans*	Yes	<0,0001
K. pneumoniae vs. *C. albicans*	No	0,0959

410

411 **Table 6.** One-way ANOVA results for comparisons of $LD_{99.9}$ and LD_{100} values of MB-
412 APDT

	LD value comparison	Significant?	Adjusted P Value
LD99.9	*E. coli vs. S. aureus*	No	>0,9999
	E. coli vs. P. aeruginosa	Yes	<0,0001
	E. coli vs. K. pneumoniae	Yes	<0,0001
	E. coli vs. C. albicans	Yes	<0,0001
	S. aureus vs. P. aeruginosa	Yes	<0,0001
	S. aureus vs. K. pneumoniae	Yes	<0,0001
	S. aureus vs. C. albicans	Yes	<0,0001
	P. aeruginosa vs. K. pneumoniae	Yes	0,0392
	P. aeruginosa vs. C. albicans	Yes	<0,0001
	K. pneumoniae vs. C. albicans	Yes	0,0150
LD100	*E. coli vs. S. aureus*	No	>0,9999
	E. coli vs. P. aeruginosa	Yes	<0,0001
	E. coli vs. K. pneumoniae	Yes	<0,0001
	E. coli vs. C. albicans	Yes	<0,0001
	S. aureus vs. P. aeruginosa	Yes	<0,0001
	S. aureus vs. K. pneumoniae	Yes	<0,0001
	S. aureus vs. C. albicans	Yes	<0,0001
	P. aeruginosa vs. K. pneumoniae	No	0,5517
	P. aeruginosa vs. C. albicans	Yes	<0,0001
	K. pneumoniae vs. C. albicans	Yes	0,0006

413

414 **Table 7.** One-way ANOVA results for comparisons of $LD_{99.9}$ and LD_{100} values of blue
415 light

	LD value comparison	Significant?	Adjusted P Value
LD99.9	*E. coli vs. S. aureus*	No	>0,9999
	E. coli vs. P. aeruginosa	Yes	0,0221
	E. coli vs. K. pneumoniae	Yes	<0,0001
	E. coli vs. C. albicans	Yes	0,0002
	S. aureus vs. P. aeruginosa	No	0,1844
	S. aureus vs. K. pneumoniae	Yes	<0,0001
	S. aureus vs. C. albicans	Yes	<0,0001
	P. aeruginosa vs. K. pneumoniae	Yes	<0,0001
	P. aeruginosa vs. C. albicans	Yes	<0,0001
	K. pneumoniae vs. C. albicans	No	>0,9999
LD100	*E. coli vs. S. aureus*	No	0,8517
	E. coli vs. P. aeruginosa	Yes	<0,0001
	E. coli vs. K. pneumoniae	Yes	<0,0001
	E. coli vs. C. albicans	Yes	<0,0001
	S. aureus vs. P. aeruginosa	Yes	0,0001
	S. aureus vs. K. pneumoniae	Yes	<0,0001
	S. aureus vs. C. albicans	Yes	<0,0001
	P. aeruginosa vs. K. pneumoniae	Yes	<0,0001
	P. aeruginosa vs. C. albicans	Yes	<0,0001
	K. pneumoniae vs. C. albicans	No	>0,9999

416
417
418